

# TRACKING A CLUSTER OF SPACE DEBRIS IN LOW ORBIT BY FILTERING ON LIE GROUPS

Samy Labsir<sup>\*†</sup>, Audrey Giremus<sup>†</sup>, Guillaume Bourmaud<sup>†</sup>, Brice Yver<sup>\*</sup> and Thomas Benoudiba–Campanini<sup>\*</sup>

<sup>\*</sup> CEA CESTA, 15 Avenue des Sablières, 33114 Le Barp cedex, France

<sup>†</sup> Université de Bordeaux, Laboratoire IMS CNRS UMR 5218, 351 cours de la Libération, 33405 Talence cedex, France

## ABSTRACT

This paper addresses the problem of tracking a cluster of space debris sufficiently close to each other to be considered as a single extended object. State-of-the-art random-matrix methods estimate the kinematics of the object centroid by assuming that its shape is elliptical and that the observations are randomly distributed within this ellipsoid. However, space debris, whose motion is driven by the gravitational force, spread out into a "banana"-like-shaped cluster. In this paper, we propose a novel Lie-group based parameterization to intrinsically capture the "banana"-like shape. More precisely, we first formulate the centroid tracking problem as filtering on Lie groups. Then, we derive an iterated extended Kalman filter on Lie groups to perform the estimation.

**Index Terms**— Space debris, Bayesian estimation, cluster tracking, manifold, filtering on Lie groups.

## 1. INTRODUCTION

The term space debris refers to natural or man-made objects which are no longer functional and are orbiting around the earth or the sun. They can be for instance pieces of meteoroids, old satellites, rocket stages or fragments from disintegrations and collisions. Space debris in low earth orbit can cause significant damages when colliding with operational spacecrafts [1][2]. Consequently, spatial surveillance has been paid a lot of attention over the past decade [3]. It consists in detecting the pieces of debris and determining their trajectories and kinematics from sensor measurements. Bayesian approaches [4] are classically used for this tracking. In addition to the measurements, they rely on a time-evolution model of the parameters of interest, gathered in a state vector. They proceed by first sequentially computing the posterior probability density function (pdf) of this state vector conditional upon all the collected measurements. Then, pointwise state estimates are derived from this pdf.

In this paper, the surveillance is based on radar measurements. Furthermore, we focus on the immediate aftermath of a fragmentation when the different pieces of debris are very close to each other and form a compact cluster. In this case, they can be considered as a single extended object and dedicated Bayesian tracking methods can be applied [5]. A target is assumed extended if it gives rise to an unknown and varying number of measurements spatially distributed within its volume. Its shape may also be unknown and evolve over time. Different algorithms have been proposed to estimate the position of the object centroid and possibly its shape. Well-known methods are the random-matrix and the star-convex shape approaches. The first category, initially proposed in [6], considers that the object is ellipsoidal and parameterized by a semi-positive definite (SPD) extent matrix. The measurements are then assumed to be normally distributed around the centroid and with a covariance directly related

to that extent matrix. Based on this model, a closed-form recursion of an approximation of the posterior pdf of both the centroid kinematic parameters and the SPD matrix is derived. However, the ellipsoidal assumption is quite restrictive. As an alternative, the second category of methods relies on a generic star-convex parametric representation of the object contour such as the random hypersurface model [7] or, more recently, the Gaussian process model [8].

The above-cited models are not well-suited for space debris in low orbit. Indeed, as the pieces of debris are only subject to the gravitational force, they were shown to spread taking a specific "banana"-like shape [1] [10]. In this work, we propose a novel random-matrix based approach that allows us to intrinsically take into account this specific contour in the tracking algorithm. Our first contribution is a new parameterization to describe the cluster of debris based on its centroid position, a rotation matrix indicating its orientation with respect to a reference frame and an SPD extent matrix. Both the centroid position and the rotation matrix can be gathered to define a state belonging to a smooth manifold, the Lie group (LG)  $SE(3)$ . Then, contrary to [6], we assume that the measurements at each time step originate from a pdf directly defined on  $SE(3)$ , which ensures the "banana"-like spreading. More precisely, we consider a concentrated Gaussian pdf centered at the unknown state and of covariance the extent matrix. An example of samples from such a distribution is given in figure 1 where the orientations are represented by the arrows attached at the position vectors. The desired "banana"-like scattering of the positions can be observed. It should be noted that it results from the joint effect of the rotation matrix and the extent matrix. As a first step, the latter is assumed to be known in this communication.

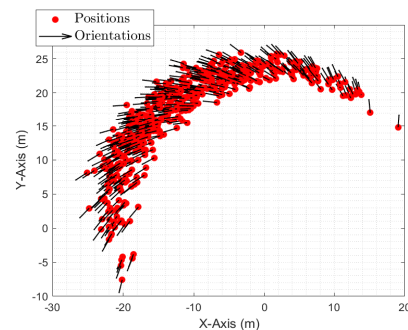


**Fig. 1.** Samples from a concentrated Gaussian pdf on the LG  $SE(3)$  projected onto the  $(X, Y)$  plane.

Finally, to solve the estimation problem thus defined, we derive an iterated extended Kalman filter on LG (LG-IEKF) that recursively computes the state estimate as the optimum of a well-chosen criterion. The algorithm proposed in [11] requires adjustments to accom-

modate the cluster tracking problem. Firstly, the centroid position is not directly sensed: instead, a set of reflector measurements randomly located within the "banana"-shaped cluster is available. Secondly, the rotation matrix is not directly observable since the radar only provides position measurements. To overcome this difficulty, we introduce auxiliary variables that have to be estimated jointly with the unknown state at the update step of the LG-IEKF. They can be interpreted as noise-free full observations that include the missing orientation information.

The communication is organized as follows. After this introduction, we provide the necessary background on LGs in section 2. In section 3, we detail the considered model and algorithm. Finally, we present some simulation results in section 4, before drawing some conclusions and perspectives in section 5.

## 2. BACKGROUND ON LIE GROUPS

In this section, we introduce the theory of LGs and the formalism of concentrated Gaussian distributions.

### 2.1. Lie group theory

A LG  $G$  is a group that has a structure of smooth manifold [13], which means that the operations of derivation and integration are smooth. In our work, we deal with matrix LGs so that  $G \subset \mathbb{R}^{n \times n}$ . Due to the smooth manifold property, we can define  $\forall g \in G$  the tangent space  $T_g G$  which corresponds to the vector space of the set of points tangent to  $G$  in  $g$ . The tangent space to the identity  $\mathbf{I}_{n \times n}$  is paid a special attention and called the Lie algebra  $\mathfrak{g}$ . The dimension  $p$  of the manifold  $G$  is the dimension of the vector space  $\mathfrak{g}$ .

The elements of  $\mathfrak{g}$  and  $G$  are linked by the exponential mapping,  $\exp_G : \mathfrak{g} \rightarrow G$ , and conversely the logarithm mapping,  $\log_G : G \rightarrow \mathfrak{g}$ . They are locally isomorphisms. For detailed expressions, the reader can refer to [11].

Furthermore, we can define an isomorphism between  $\mathfrak{g}$  and the Euclidean space  $\mathbb{R}^p$ . If  $\mathbf{a}$  is an element of  $\mathbb{R}^p$  and  $\mathfrak{a}$  its image in  $\mathfrak{g}$ , we denote  $\mathfrak{a} = [\mathbf{a}]_G^\wedge$  and  $\mathbf{a} = [\mathfrak{a}]_G^\vee$  respectively. The relationship between the LG, its algebra and the related Euclidean space are represented in figure 2. For the sake of simplicity, in the following, we use the condensed notations  $\mathfrak{a} = \log_G^\vee(X) = [\log_G(X)]^\vee$  and  $X = \exp_G^\wedge(\mathfrak{a}) = \exp_G([\mathfrak{a}]_G^\wedge)$ , with  $X \in G$  and  $\mathfrak{a} \in \mathbb{R}^p$ .

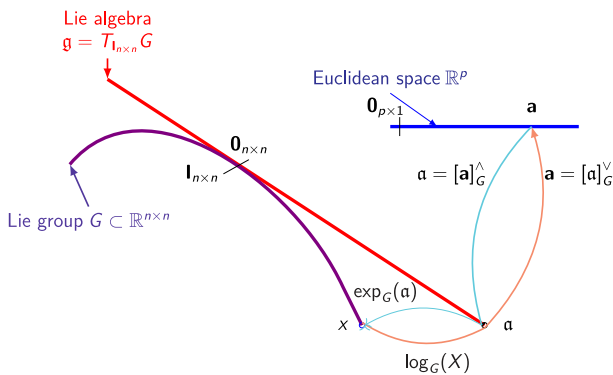


Fig. 2. Link between  $G$ ,  $\mathfrak{g}$  and  $\mathbb{R}^p$

Examples of matrix Lie groups:

- $SO(n) = \{\mathbf{P} \in GL(n) \mid \mathbf{P} \cdot \mathbf{P}^T = \mathbf{I}_n, |\mathbf{P}| = 1\}$ , where  $GL(n)$  refers to the group of the invertible matrices of di-

mension  $n$ : equipped with the law  $\cdot$ , the neutral  $\mathbf{I}_n$  and the inverse operator  $()^{-1}$ .

- $SE(n) = \left\{ \begin{bmatrix} \mathbf{A} & \mathbf{x} \\ \mathbf{0}_{1 \times n} & 1 \end{bmatrix} \mid \mathbf{A} \in SO(n), \mathbf{x} \in \mathbb{R}^n \right\}$ : equipped with the law  $\cdot$ , the neutral  $\begin{bmatrix} \mathbf{I}_n & \mathbf{0}_{n \times 1} \\ \mathbf{0}_{1 \times n} & 1 \end{bmatrix}$  and the inverse operator  $()^{-1}$ .

### 2.2. Concentrated Gaussian distribution

In a Bayesian framework, the estimators are built from the posterior distribution of the unknown parameters. When the latter evolve on LGs, it is thus crucial to define pdfs that intrinsically account for this constraint. In [12] and [14], the formalism of concentrated Gaussian probability pdfs was introduced. It makes it possible to represent uncertainty directly on LGs. First of all, let  $\mathcal{N}(\mathbf{x}; \mathbf{m}, \mathbf{\Sigma})$  denote the multivariate Gaussian pdf with mean  $\mathbf{m}$  and covariance matrix  $\mathbf{\Sigma}$  computed at vector  $\mathbf{x}$ . If  $\epsilon \sim \mathcal{N}(\epsilon; \mathbf{0}_{p \times 1}, \mathbf{P})$ , then  $X = \mu \exp_G^\wedge(\epsilon)$  is distributed according to a left concentrated Gaussian pdf on a LG  $G$ , with mean  $\mu \in G$  and covariance  $\mathbf{P} \in \mathbb{R}^{p \times p}$ . We denote  $X \sim \mathcal{N}_G^L(X; \mu, \mathbf{P})$ . In the neighborhood of  $\mu$ , the expression of this pdf can be approximated by:

$$p(X) = \frac{1}{\sqrt{(2\pi)^p |\mathbf{P}|}} \exp^{-\frac{1}{2} \|\log_G^\vee(\mu^{-1} X)\|_{\mathbf{P}}^2}, \quad (1)$$

where  $|\mathbf{P}|$  is the determinant of the matrix  $\mathbf{P}$  and  $\|\cdot\|_{\mathbf{P}}^2$  the Mahalanobis distance.

## 3. PROPOSED APPROACH

As mentioned in the literature [1][10], we could observe by numerical simulations that a group of objects whose motion is completely driven by the gravitational force tends to spread taking a specific configuration illustrated in figure 3. The latter is typical of samples distributed according to concentrated Gaussian pdfs on some LGs. This work proposes a novel approach to track a cluster of space debris complying with this property. For that purpose, we represent the cluster by both the centroid position and an orientation with respect to the earth centered earth fixed (ECEF) frame used as a reference for the tracking. The latter takes the form of a rotation matrix between the ECEF frame and a local frame attached to the centroid. Both the centroid position and cluster rotation matrix form a state belonging to the LG  $SE(3)$  and propagating with the desired "banana"-shaped uncertainty. In this section, we formulate the estimation of the cluster state from the collected measurements as a filtering problem on LG. We first present the considered state space representation to ensure that both the state and the measurements lie on LGs. Then, we derive an algorithm to solve the estimation problem. It builds upon the LG-IEKF introduced in [11] but with a different update step. Indeed, the specificity is that the cluster gives rise at each time step to several measurements randomly scattered within its volume.

### 3.1. State model

The state of the cluster is described by the matrix  $M_k = \begin{bmatrix} \mathbf{R}_k & \mathbf{p}_k \\ \mathbf{0}_{1 \times 3} & 1 \end{bmatrix}$  in  $SE(3)$  with  $\mathbf{p}_k$  and  $\mathbf{R}_k$  the position of its centroid and its rotation matrix, respectively.

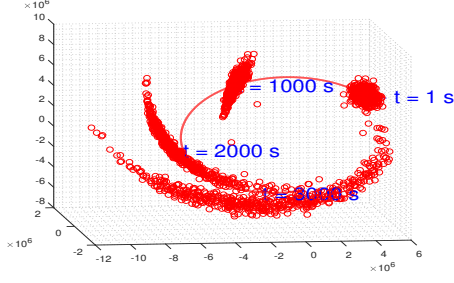


**Fig. 3.** Temporal evolution of cluster of space debris by Monte-Carlo simulation.

However, the evolution of  $\mathbf{p}_k$  under the influence of the gravitational force depends on the previous velocity  $\mathbf{v}_{k-1}$  which is itself unknown. Therefore, we have to consider a state augmented by  $\mathbf{v}_k$  which belongs to  $\mathbb{R}^3$ . By noting that  $\mathbb{R}^3$  can be considered as a  $SE(3)$  LG with a rotation matrix fixed at the identity, we propose the following state in the LG  $SE(3) \times \mathbb{R}^3$ :

$$X_k = \begin{bmatrix} M_k & \mathbf{0}_{6 \times 6} \\ \mathbf{0}_{4 \times 4} & \mathbf{I}_{3 \times 3} & \mathbf{v}_k \\ & \mathbf{0}_{1 \times 3} & 1 \end{bmatrix}.$$

For the sake of brevity, we denote in the sequel  $G = SE(3) \times \mathbb{R}^3$ .

### 3.1.1. Position and velocity components

The dynamic model for the position and velocity is obtained thanks to Newton's first law [1]. After discretization, it can be written as the following set of stochastic difference equations:

$$\mathbf{p}_k = \underbrace{\mathbf{p}_{k-1} + T_e \mathbf{f}_p(\mathbf{p}_{k-1}, \mathbf{v}_{k-1})}_{\tilde{\mathbf{f}}_p(\mathbf{p}_{k-1}, \mathbf{v}_{k-1})} + \mathbf{w}_{p,k}, \quad (2)$$

$$\mathbf{v}_k = \underbrace{\mathbf{v}_{k-1} + T_e \mathbf{f}_v(\mathbf{p}_{k-1}, \mathbf{v}_{k-1})}_{\tilde{\mathbf{f}}_v(\mathbf{p}_{k-1}, \mathbf{v}_{k-1})} + \mathbf{w}_{v,k}, \quad (3)$$

with  $\mathbf{f}_p$  and  $\mathbf{f}_v$  two non-linear functions depending on the earth mass and its angular velocity and  $T_e$  the sampling period. As for  $\mathbf{w}_{p,k}$  and  $\mathbf{w}_{v,k}$ , they are respectively the position and velocity noises, due to unexpected disturbances (lunar attraction, solar winds, ...) and uncertainties on the physical model. They are assumed to be centered and normally distributed.

### 3.1.2. Rotation matrix

We assume the evolution of  $\mathbf{R}_k$  is a random walk on the LG  $SO(3)$  defined in section 2:

$$\mathbf{R}_k = \mathbf{R}_{k-1} \exp_{SO(3)}^{\wedge}(\mathbf{w}_{R,k}) \quad (4)$$

where  $\mathbf{w}_{R,k}$  is zero-mean and normally distributed.

By concatenating (2), (3) and (4), we can rewrite in compact form:

$$X_k = f_k(X_{k-1}) \exp_G^{\wedge}(\mathbf{w}_k), \quad (5)$$

with

$$f_k(X_{k-1}) = \begin{bmatrix} \mathbf{R}_{k-1} & \tilde{\mathbf{f}}_p(\mathbf{p}_{k-1}, \mathbf{v}_{k-1}) & \mathbf{0}_{3 \times 3} & \mathbf{0}_{3 \times 3} \\ \mathbf{0}_{1 \times 3} & 1 & \mathbf{0}_{1 \times 3} & \mathbf{0}_{1 \times 3} \\ \mathbf{0}_{3 \times 3} & \mathbf{0}_{3 \times 3} & \mathbf{I}_{3 \times 3} & \tilde{\mathbf{f}}_v(\mathbf{p}_{k-1}, \mathbf{v}_{k-1}) \\ \mathbf{0}_{1 \times 3} & \mathbf{0}_{1 \times 3} & \mathbf{0}_{1 \times 3} & 1 \end{bmatrix}$$

and  $\mathbf{w}_k = [\mathbf{w}_{R,k}^T, \mathbf{w}_{p,k}^T, \mathbf{w}_{v,k}^T]^T$  with  $\mathbf{w}_k \sim \mathcal{N}(\mathbf{w}_k; \mathbf{0}, \mathbf{W}_k)$ .

## 3.2. Measurement model

At time  $k$ , not all the objects within the cluster are detected by the radar sensor. Only a part of them, denoted  $n_k$ , are reflectors. To capture this behavior, we assume they spread around the centroid  $M_k$  according to the concentrated Gaussian model:

$$Z_{k,i} = M_k \exp_{SE(3)}^{\wedge}(\boldsymbol{\epsilon}_{k,i}), \text{ for } i = 1, \dots, n_k, \quad (6)$$

which ensures the "banana"-like scattering.  $\boldsymbol{\epsilon}_{k,i} \sim \mathcal{N}(\boldsymbol{\epsilon}_{k,i}; \mathbf{0}, \mathbf{S}_k)$  with  $\mathbf{S}_k$  the cluster extent matrix.

However, the radar only provides position measurements so that the orientations of the reflectors are not directly observable. The actual measurements take the form:

$$\mathbf{z}_{k,i} = \Pi(Z_{k,i}) + \mathbf{u}_{k,i}, \quad (7)$$

where for  $i = 1, \dots, n_k$ ,  $\mathbf{u}_{k,i}$  is the observation noise that satisfy  $\mathbf{u}_{k,i} \sim \mathcal{N}(\mathbf{u}_{k,i}; \mathbf{0}, \mathbf{U}_k)$ . As for  $\Pi : SE(3) \rightarrow \mathbb{R}^3$ , it is a mapping which projects the Euclidean part of an element of  $SE(3)$ .

In the rest of the paper, we denote  $\mathbf{z}_k = \{\mathbf{z}_{k,i}\}_{i=1}^{n_k}$ , the set of reflector measurements at time  $k$ .

## 3.3. Proposed algorithm

To jointly address the model non-linearities and intrinsically take into account the LG properties, an LG-IEKF approach [11] is considered for the estimation. This variant of the extended Kalman filter on LG [12] approximates the posterior pdf of interest by a concentrated Gaussian on LGs, but the prediction and the correction steps are rewritten as optimization problems. The two minimizers provide the predicted and the corrected states respectively, and the posterior covariance matrices are obtained by a Gauss-Laplace approximation on LG [11]. Classically, a Gauss-Newton (GN) algorithm is used to perform these optimizations.

### 3.3.1. Prediction step

In this step, the aim is to approximate the posterior distribution  $p(X_k | \mathbf{z}_1, \dots, \mathbf{z}_{k-1})$  by a left concentrated Gaussian pdf  $\mathcal{N}_G^L(X_k; \mu_{k|k-1}, \mathbf{P}_{k|k-1})$  and then take the mean  $\mu_{k|k-1}$  as the state estimate. Following [10], the joint estimate of the couple  $\{X_k, X_{k-1}\}$  is obtained by solving:

$$\begin{aligned} \{\hat{X}_{k|k-1}, \hat{X}_{k-1}\} = \arg \min_{X, \tilde{X}} & \|\log_G^{\vee}(f_k(\tilde{X})^{-1} X)\|_{\mathbf{W}_k}^2 \\ & + \|\log_G^{\vee}(\mu_{k-1}^{-1} \tilde{X})\|_{\mathbf{P}_{k-1}}^2, \end{aligned} \quad (8)$$

where  $\mu_{k-1}$  and  $\mathbf{P}_{k-1}$  are respectively the mean and the covariance matrix of the estimated posterior distribution at the previous time step  $p(X_{k-1} | \mathbf{z}_1, \dots, \mathbf{z}_{k-1}) = \mathcal{N}_G^L(X_{k-1}; \mu_{k-1}, \mathbf{P}_{k-1})$ . The solution is trivial for  $\hat{X}_{k-1} = \mu_{k-1}$  and corresponds to propagating the state estimate through the dynamic equations without noise for  $\hat{X}_{k|k-1} = \mu_{k|k-1} = f_k(\mu_{k-1})$ . Its components are expressed as:

$$\hat{\mathbf{p}}_{k|k-1} = \tilde{\mathbf{f}}_p(\hat{\mathbf{p}}_{k-1}, \hat{\mathbf{v}}_{k-1}) \quad (9)$$

$$\hat{\mathbf{v}}_{k|k-1} = \tilde{\mathbf{f}}_v(\hat{\mathbf{p}}_{k-1}, \hat{\mathbf{v}}_{k-1}) \quad (10)$$

$$\hat{\mathbf{R}}_{k|k-1} = \hat{\mathbf{R}}_{k-1}. \quad (11)$$

The predicted covariance is given by:

$$\mathbf{P}_{k|k-1} = \mathbf{F}_k \mathbf{P}_{k-1} \mathbf{F}_k^T + \mathbf{W}_k \quad (12)$$

where  $\mathbf{F}_k = \frac{df_k(\hat{X}_{k-1} \exp_G^{\wedge}(\boldsymbol{\delta}))}{d\boldsymbol{\delta}}|_{\boldsymbol{\delta}=\mathbf{0}}$  is the Jacobian matrix of  $f_k$  evaluated at  $\hat{X}_{k-1}$ .

### 3.3.2. Correction step

In this step, the aim is to approximate the posterior pdf  $p(X_k | \mathbf{z}_1, \dots, \mathbf{z}_k)$  by a left concentrated Gaussian pdf  $\mathcal{N}_G^L(X_k; \mu_k, \mathbf{P}_k)$ . As in the prediction step,  $\mu_k$  is considered for the state estimate  $\hat{X}_k$ . The difficulty in our context is that  $X_k$  is indirectly related to the observations through the matrices  $Z_k = \{Z_{k,i}\}_{i=1}^{n_k}$ . Thus, we choose to handle them as latent variables that have to be estimated jointly with  $X_k$ . Then, the estimates  $\{\hat{X}_k, \hat{Z}_k\}$  are computed by minimizing the opposite of the logarithm of the posterior pdf:

$$J(X_k, Z_k) = \sum_{i=1}^{n_k} \left( \|\mathbf{z}_{k,i} - \Pi(Z_{k,i})\|_{\tilde{\mathbf{U}}_k}^2 + \|\log_{SE(3)}^\vee(M_k^{-1} Z_{k,i})\|_{\tilde{\mathbf{S}}_k}^2 \right) + \|\log_G^\vee(\mu_{k|k-1}^{-1} X_k)\|_{\mathbf{P}_{k|k-1}}^2. \quad (13)$$

We rewrite it compactly  $J(X_k, Z_k) = \|\psi(X_k, Z_k)\|_{\Sigma_k}^2$ , where  $\Sigma_k = \text{blkdiag}(\tilde{\mathbf{U}}_k, \tilde{\mathbf{S}}_k, \mathbf{P}_{k|k-1})$  with  $\tilde{\mathbf{U}}_k = \mathbf{I}_{n_k} \odot \mathbf{U}_k$ ,  $\tilde{\mathbf{S}}_k = \mathbf{I}_{n_k} \odot \mathbf{S}_k$ , and the notations  $\odot$  and  $\text{blkdiag}$  referring to the Kronecker product and a block diagonal matrix respectively. The minimization of the criterion is carried out with the GN algorithm and the corrected covariance error  $\mathbf{P}_k$  is obtained by the Gauss-Laplace approximation in two steps:

1/ The covariance of the joint posterior distribution of  $\{X_k, Z_k\}$  is estimated by

$$\mathbf{C}_k = (\mathbf{J}_l^T \Sigma_k^{-1} \mathbf{J}_l)^{-1}, \quad (14)$$

where  $\mathbf{J}_l$  corresponds to the LG Jacobian matrix of  $\psi$  at the  $l^{\text{th}}$  iteration of GN. The latter is derived using formula of derivatives on LG. 2/ Only the components of  $\mathbf{C}_k$  corresponding to elements of  $X_k$  are selected to yield  $\mathbf{P}_k$ .

## 4. SIMULATION RESULTS

We validate the proposed approach by considering a cluster of spatial objects evolving in low orbit so that each of them is located at an altitude ranging from  $10^5$  to  $10^6$  m. The initial velocity of the centroid is chosen close to  $10^3$  m s<sup>-1</sup>. The velocity, position and orientation standard deviations appearing in the state models (2), (3) and (4) are fixed respectively with a value equal to 1 m, 1 m s<sup>-1</sup> and  $10^{-4}$  rad. Furthermore, the sampling period of trajectory  $T_e$  is taken small, i.e. equal to  $10^{-2}$  s. As for the reflector measurements, they are directly generated according to the models (6) and (7) with a covariance matrix  $\mathbf{S}_k$  which is assumed in this preliminary work to be known and time-invariant. Finally, a mean number of 70 reflectors is considered except when it is varied to study the impact on the estimation error. The obtained estimation results are presented in figure 4 wherein mean errors are computed by averaging  $N = 50$  MC runs. In figure 4-(a), we plot the true trajectory of the centroid of the "banana"-shape, the estimated one, as well as the cluster of measurements, respectively in blue, red and black. For the sake of clarity, only the time instants 100 s, 200 s, 300 s and 500 s are represented. In spite of an initial error of the order of  $10^4$  m, we can observe that the true position of the centroid is recovered in a few iterations. To better validate the robustness to significant initial position errors, we represent the global position root mean square error RMSE all along the trajectory for different initializations in 4-(b). We can observe that the final RMSE remains inferior to 10 m even if the first guess

is  $10^4$  meters away from the true centroid position. Furthermore, the figure 4-(c) shows an example of the convergence of the GN algorithm implemented at each iteration of the correction step of the filter. It can be noted that it converges in a few iterations in conjunction to a small value of the state estimation error computed directly on the LG as  $\|\log_G^\vee(X_k^{-1} \hat{X}_k)\|_2^2$ . Finally, in figure 4-(d), we test the influence of the number of reflectors. When it is superior to 70, the global position RMSE computed over all the trajectory becomes inferior to 10 m.

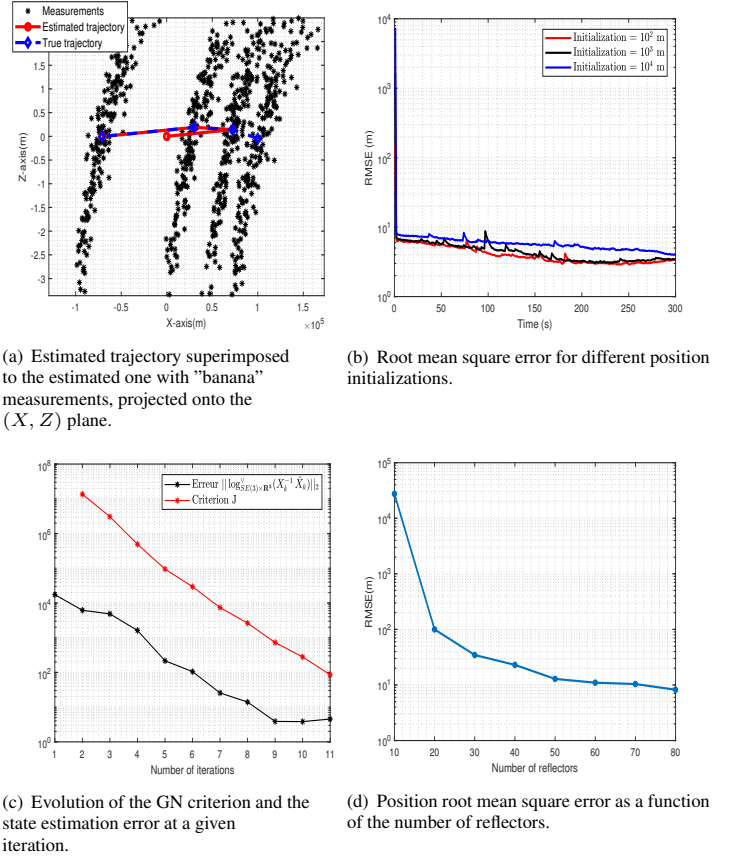


Fig. 4. Obtained results

## 5. CONCLUSIONS AND PERSPECTIVES

In this paper, we proposed a novel model and algorithm to recursively estimate the trajectory and the dynamics of the centroid of a cluster of space debris spreading according to a "banana"-like shape. We formalize the problem as a filtering problem on LG to obtain a set of measurements spatially distributed according to this specific configuration. The proposed algorithm to perform the estimation is a variant of the LG-IEKF where the update step was modified to address the tracking of an extended object. A perspective is to include the estimation of the SPD extent matrix in the algorithm. By using an eigenvalue decomposition, the latter can indeed be reparameterized to belong to a LG so that the presented formalism is well-suited to also address this issue.

## 6. REFERENCES

- [1] H. Klinkrad, Space debris, Wiley Online Library, 2010.
- [2] The Threat of Orbital Debris and Protecting NASA Space Assets from Satellite Collisions, NASA, 28 April 2009.
- [3] J.A. Kennewell and B.-N. Vo, An overview of space situational awareness, 16th International Conference on Information Fusion, Istanbul, Turkey, July 2013.
- [4] S. Arulampalam, S. Maskell, N. Gordon and T. Clapp, A Tutorial on Particle Filter for Online Nonlinear/Non-Gaussian Bayesian Tracking, IEEE Transactions on Signal Processing, vol 50, 2002.
- [5] K. Granstrom, M. Baum and S. Reuter, Extended Object Tracking: Introduction, Overview and Applications, Journal of Advances in Information Fusion, 2017.
- [6] J.W. Koch, Bayesian Approach to Extended Object and Cluster Tracking Using Random Matrices, IEEE Transactions on Aerospace and Electronic Systems, Vol 44, 2008.
- [7] M. Baum and U.D. Hanebeck, Extended Object Tracking with Random Hypersurface Models, IEEE Transactions on Aerospace and Electronic Systems, 2014, 50, 149-159.
- [8] N. Wahlström and E. Özkan, Extended Target Tracking Using Gaussian Processes, IEEE Transactions on Signal Processing, vol. 63, no.16, August 2015.
- [9] J.E. Prussing and B.A. Conway, Orbital Mechanics, Oxford University Press, USA, 1993.
- [10] J.T. Horwood and A.B. Poore, Orbital State Uncertainty Realism, Proceedings of the Advanced Maui Optical and Space Surveillance Technologies Conference, September 2011.
- [11] G. Bourmaud, R. Mégret, A. Giremus and Y. Berthoumieu, From Intrinsic Optimization to Iterated Extended Kalman Filtering on Lie Groups, Journal of Mathematical Imaging and Vision, Springer Verlag, 2016, 55(3).
- [12] G. Bourmaud, R. Mégret, M. Arnaudon and A. Giremus, Continuous-Discrete Extended Kalman Filter on Matrix Lie groups, Journal of Mathematical Imaging and Vision, January 2015, Volume 51
- [13] A. Baker, Matrix Groups: an Introduction to Lie Group Theory, Springer, 2003.
- [14] T.D. Barfoot and P. T. Furgale, Associating Uncertainty With Three-Dimensional Poses for Use in Estimation Problem, IEEE Transactions on Robotics, June 2014.